Image-Based Spectral Reflectance Reconstruction Using the Matrix R Method

Yonghui Zhao, Roy S. Berns*

Munsell Color Science Laboratory, Chester F. Carlson Center for Imaging Science, Rochester Institute of Technology, Rochester, NY

Received 24 April 2006; revised 27 September 2006; accepted 27 October 2006

Abstract: The ultimate goal of spectral imaging is to achieve high spectral accuracy, so that the spectral information can be used to calculate colorimetrically accurate images for any combination of illuminant and observer. A new spectral reconstruction method, called the matrix R method, was developed to reconstruct spectral reflectance factor accurately while simultaneously achieving high colorimetric performance for a defined illuminant and observer. The method combines the benefits of both colorimetric and spectral transformations. Tristimulus values were predicted by a colorimetric transformation from multi-channel camera signals, while spectral reflectance factor was estimated by a spectral transformation from the same signals. The method reconstructed reflectance factor by combining the fundamental stimulus from the predicted tristimulus values with the metameric black from the estimated spectral reflectance, based on the Wyszecki hypothesis. The experimental results verified the new method as a promising technique for building a spectral image database. © 2007 Wiley Periodicals, Inc. Col Res Appl, 32, 343–351, 2007; Published online in Wiley InterScience (www.interscience.wiley.com). DOI 10.1002/col.20341

Key words: matrix R; Wyszecki hypothesis; spectral imaging; metamerism

INTRODUCTION

Imaging is an important technique for the visual documentation of cultural heritage. There is an urgent need to build digital-image databases with adequate colorimetric accuracy for museums, archives, and libraries. Conventional color-acquisition devices capture spectral signals by acquiring only three samples, critically under-sampling spectral information and suffering from metamerism. Alternatively, spectral devices increase the number of samples and can reconstruct spectral information for each scene pixel. Retrieving the spectral reflectance factor of each pixel is highly desirable, since spectral information can be used to calculate colorimetrically accurate images for any combination of illuminant and observer. The advantages of spectral imaging have been summarized in Refs. 1–16. Spectral imaging has been widely developed over the last 10 years at a number of institutions worldwide, for example, at the National Gallery, London in the United Kingdom,[2,3] ENST Paris in France,[4–6] Aachen University of Technology in Germany,[7–9] the University of Joensuu in Finland,[10] Chiba University and Osaka Electro-Communication University in Japan,[11–13] and Rochester Institute of Technology in the United States.[14–16]

The reflectance reconstruction techniques can be classified into three categories: direct reconstruction, reconstruction by interpolation, and indirect reconstruction or learning-based reconstruction.[4] First, direct reconstruction is based on the inverse of the overall spectral sensitivity of a camera system, which is a matrix multiplication of the spectral distribution of the light source, the spectral transmittances of the color filters and the spectral response of the sensor.[11] Second, the camera responses can be interpolated to find an approximation of the corresponding spectral reflectance factor, and therefore the method is called reconstruction by interpolation. For the EU-funded CRISATEL project, a spectral acquisition system had 10 interference filters in the visible range and three in the near-infrared range, and spectral reflectance factor was reconstructed by a simple cubic-spline interpolation between measured points.[3] The system exhibited high spectral and colorimetric accuracies. Finally, indirect

*Correspondence to: Roy S. Berns (e-mail: berns@cis.rit.edu).

Contract grant sponsors: Andrew W. Mellon Foundation, National Gallery of Art (Washington), Museum of Modern Art (New York), Institute of Museum and Library Services (IMLS), Rochester Institute of Technology.

reconstruction is also called learning-based reconstruction. It means that a calibration target is first used to build the transform between camera signals and spectral reflectance factor, and after that, camera signals of other targets can be transferred into spectral reflectance factor. A multi-year research program at the Munsell Color Science Laboratory (MCSL) at Rochester Institute of Technology was developed to implement many methods of spectral color reproduction based on this learning process.[14] Three multispectral acquisition systems were developed and tested: a liquid-crystal tunable filter with a monochrome camera, six absorption filters with a monochrome camera, and two absorption filters with a commercial color-filter-array (CFA) camera.[14–16] The last system was the most practical system and was used as the spectral imaging-acquisition system in this research.

A new spectral reconstruction method, to be referred to as the "matrix R method," was developed based on Wyszecki hypothesis and the matrix R theory developed by Cohen and Kappauf, described in detail below. The major advantage of the new method is to reconstruct spectral reflectance factor accurately while simultaneously achieving high colorimetric performance for a defined viewing and illuminating condition. This method belongs to a learning-based reconstruction, i.e., a calibration target is required to build the camera model. Spectral reflectance factors of the target are estimated from camera signals using the linear-least-squares (LLS) method to minimize spectral root-mean-square (RMS) error. Concomitantly, tristimulus values of the target are predicted from the same camera signals using nonlinear optimization to minimize color differences for a defined illuminant and observer. The matrix R method can be used to generate spectra by combining the "fundamental stimuli" from the predicted tristimulus values with the "metameric blacks" from the estimated spectral reflectance factors based on the Wyszecki hypothesis. Thus the method merges the benefits from both colorimetric and spectral transformations.

MATRIX R THEORY

Metamerism is fundamental to basic colorimetry. Many imaging techniques used for color imaging reproduction are inherently metameric. For example, reproduced color images on a television have spectral radiance distributions that show little or no similarity to those of the original scene, but result in the same perceived color appearance.[17] In 1953, Wyszecki hypothesized that any color stimulus can be decomposed into two spectra, a "fundamental stimulus" and a "metameric black."[18] The tristimulus values of the metameric black are, by definition, 0,0,0 and the fundamental stimulus carries all the tristimulus information of a color stimulus. It is "fundamental" because the human visual system is only processing this portion of the incident spectrum. The Wyszecki hypothesis gives an alternative explanation of metamerism, which is a property of two stimuli that have identical fundamental stimuli but different metameric blacks under a reference condition.[19]

Based on the Wyszecki hypothesis, Cohen and Kappauf developed a mathematical technique for decomposing the color stimulus into its fundamental and metameric black, often referred to as spectral decomposition theory or matrix R theory.[20–23] The terms, symbols, and definitions from the Refs. 19 and 24 will be adopted herein. The critical aspect of matrix R theory is actually an orthogonal projector, called matrix **R**. This matrix is calculated from matrix **A**, which represents a weight set for tristimulus integration applicable to a defined combination of illuminant and observer. Matrix **A** is an *n*-by-*3* matrix where *n* is the number of wavelength intervals and the three columns are three independent primaries. Matrix **R**, an *n*-by-*n* symmetric matrix, is mathematically defined in Eq. (1), where the prime mark means matrix transpose and the superscript (-1) means matrix inverse. The diagonal of matrix **R** has been used as the weighting function of spectral root-mean-square error in order to minimize both spectral and colorimetric errors simultaneously.[25]

$$\mathbf{R} = \mathbf{A}(\mathbf{A}'\mathbf{A})^{-1}\mathbf{A}' \tag{1}$$

The projection matrix **R** can be used to decompose any stimulus. A stimulus could be the spectral reflectance or transmittance of a specimen or the spectral radiance or irradiance of a source, represented by an *n*-by-1 column vector **N**. The fundamental stimulus **N***, an *n*-by-1 column vector, is the orthogonal projection of **N** on matrix **R**, shown in Eq. (2). The metameric black **B** is the residual between **N** and **N*** [Eq. (3)], and can also be calculated by substituting Eq. (2) into Eq. (3), where **I** is an *n*-by-*n* identity matrix, as shown in Eq. (4).

$$\mathbf{N}^* = \mathbf{RN} \tag{2}$$

$$\mathbf{B} = \mathbf{N} - \mathbf{N}^* \tag{3}$$

$$\mathbf{B} = (\mathbf{I} - \mathbf{R})\mathbf{N} \tag{4}$$

It can be derived that **N** and **N*** share the same fundamental stimulus since the orthogonal projector has the property of $\mathbf{R}^2 = \mathbf{R}'$, i.e., **N** and **N*** form a metameric pair. Because **N** and **N*** have the same tristimulus values, the tristimulus values for **B** are zero, hence the term "metameric black". Also, the fundamental stimulus **N*** can be calculated from a 3-by-1 column vector **T** of tristimulus values, derived from Eqs. (1), (2), and (5) and shown in Eq. (6). The *n*-dimensional spectral space is decomposed into a three-dimensional human-visual-system subspace and a (*n*-3)-dimensional metameric-black space.[26]

$$\mathbf{T} = \mathbf{A}'\mathbf{N} \tag{5}$$

$$\mathbf{N}^* = \mathbf{A}(\mathbf{A}'\mathbf{A})^{-1}\mathbf{T} \tag{6}$$

Matrix R theory has been used in several applications. Fairman proposed a method to correct paramers using the theory.[27] Differing from metamers, paramers have approximately equal fundamental stimuli and different metameric blacks. For a parameric pair, one is called the standard specimen and the other is the trial specimen. The spectral stimuli of both the standard and trial specimens are decomposed into their fundamental stimuli and metameric blacks. The trial specimen is corrected by replacing its fundamental stimulus with that of the standard specimen while retaining its metameric black. So the corrected and standard specimens become a metameric pair. The index of metamerism for paramers is the color difference under the test viewing condition calculated based on the corrected trial and standard specimens. An illustrative example was given in Ref. 28.

Imai and Berns combined images captured at different resolutions based on the theory.[29] High-resolution lightness information was obtained from a scanned high-resolution photographic image. Spectral reflectance factor and colorimetric values were estimated from a low-resolution multi-channel camera image. Image fusion was performed on the high-resolution lightness information and low-resolution colorimetric values since the human visual system is more sensitive to achromatic than to chromatic spatial information. The fused CIELAB image was transformed to an XYZ (tristimulus values) image and then an **N***(fundamental stimulus) image. The hybrid image combined the metameric blacks from the estimated spectral reflectance factors and the fundamental stimuli from the fused image. Thus, a high-resolution photographic image was combined with a low-resolution multispectral image to generate the high-resolution spectral image. The two applications above share a common point that fundamental stimuli and metameric blacks are generated from different sources and then combined based on matrix R theory.

The orthogonal projector of matrix **R** can be generalized to matrix **S**, where **E** is an *n*-by-3 matrix, as shown in Eq. (7).[27]

$$\mathbf{S} = \mathbf{E}(\mathbf{A}'\mathbf{E})^{-1}\mathbf{A}' \tag{7}$$

Matrix **E** defines the spectra of a three-primary additive color system. Linear combinations of these spectra weighted by their scalar amounts result in a fundamental stimulus. When $\mathbf{E} = \mathbf{A}$, then $\mathbf{S} = \mathbf{R}$. In this case the spectra of the additive color system are tristimulus integration weights and the fundamental stimulus is a linear combination of these tristimulus integration weights. Given that the CIE XYZ system was arbitrary and defined in order to solve practical computational limitations in 1931, it is arguable whether the fundamental stimulus calculated with Eq. (2) is, in fact, "fundamental." Recently, alternative primaries were derived using principal component analysis and independent component analysis from ensembles of spectral reflectance factors from both the *Munsell Book of Color* and an automotive paint system. These primaries were found to be significantly better than tristimulus integration weights when used to correct paramers computationally that approximated batch correction.[30] Thus, although we do not advocate that matrix **R** identifies **the fundamental**, this terminology was adopted in this publication because of its common usage.

The theory also finds application in spectral color management.[31] Traditional color management uses the human visual system as its profile connection space (PCS), while spectral color management uses the six-dimensional LabPQR as its interim connection space (ICS). The LabPQR includes three colorimetric dimensions (CIELAB) and three approximate metameric black dimensions (PQR). Spectral reflectance factor can be transformed to and roughly predicted from the LabPQR values. Although the formation of fundamental stimuli and metameric blacks are totally innovative, the underlying idea of the LabPQR is comparable to matrix R theory.

Finally, matrix R theory finds its new application in spectral imaging. The resulting spectral reconstruction method is referred to as the matrix R method, the subject of this publication.

MATRIX R METHOD

The matrix R method combines the fundamental stimulus from a colorimetric transformation with the metameric black from a spectral transformation.

A spectral transformation can be derived to convert multi-channel camera signals, **D**, for a color target to spectral reflectance factor, **N**, as shown in Eq. (8). The transformation matrix, $\mathbf{M_s}$, is the optimal solution to this unconstrained linear-least-squares (LLS) problem based on a specific calibration target, shown in Eq. (9):

$$\mathbf{N} = \mathbf{M_s}\mathbf{D} \tag{8}$$

$$\mathbf{M_s} = \mathbf{N} \times \mathbf{PINV}(\mathbf{D}) \tag{9}$$

where **PINV(D)** means the Moore-Penrose pseudoinverse of matrix **D**. After the derivation of the transformation matrix $\mathbf{M_s}$, the spectral reflectances for any other target can be calculated, and the estimated reflectances are expressed as $\hat{\mathbf{N}}$ (in order to differentiate from the measured reflectances **N**). For example, for a six-channel camera and the use of a GretagMacbeth ColorChecker DC as the calibration target (that has 240 patches), the measured spectral reflectances, **N**, is an *n*-by-240 matrix (*n* is the number of wavelengths) and the corresponding 6-channel camera signals, **D**, is a 6-by-240 matrix, so the resulting transform matrix, $\mathbf{M_s}$, is an *n*-by-6 matrix. Since the transformation matrix is an unconstrained solution, the reconstructed reflectances might be negative, in which case these values will be defined as zero. This limitation can be minimized by two improved approaches. One is to generate a new transformation matrix, each column of which is a basis vector of a reflectance database, as discussed in Ref. 30. The other approach is to adding some kind of physical constraint. For example, if pigment compositions of a painting can be solved on pixel basis, the reflectance can be reconstructed by incorporating pigment information, which will guarantee the physical property of reflectance.[32] This simple spectral reconstruction method will be referred to as the pseudoinverse method.

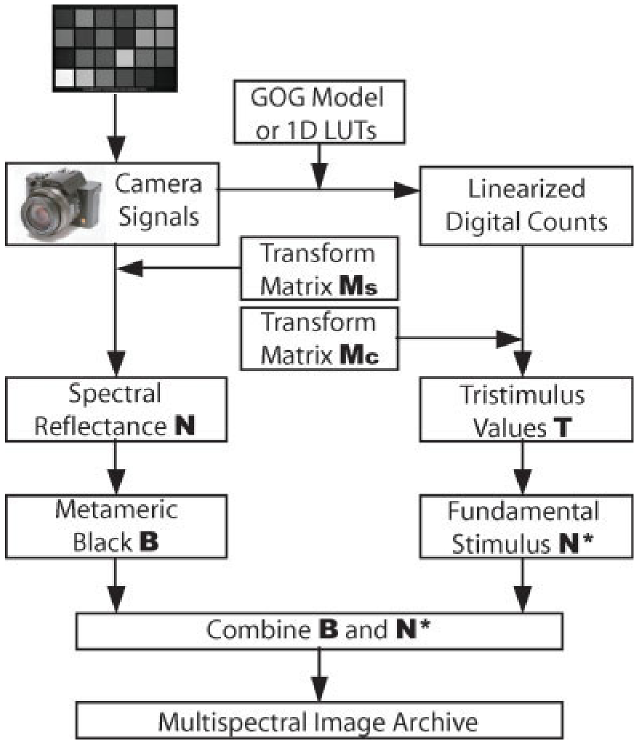

FIG. 1. Flowchart of the matrix R method. [Color figure can be viewed in the online issue, which is available at www.interscience.wiley.com.]

On the other hand, a colorimetric transformation can be derived to convert camera signals to tristimulus values. Similar to commercial profiling software, a camera profile is generated by first linearizing the camera signals to photometric data, followed by a matrix multiplication. The camera signals for each channel were corrected using the gain-offset-gamma (GOG) model, commonly used to characterize CRT displays,[33] and then converted to tristimulus values:

$$\mathbf{D}_{\mathbf{L},\mathbf{i}} = (\alpha_i \mathbf{D}_\mathbf{i} + \beta_i)^{\gamma_i} \tag{10}$$

$$\mathbf{T} = \mathbf{M}_\mathbf{c}\mathbf{D}_\mathbf{L} \tag{11}$$

where $\mathbf{D}_{\mathbf{L},\mathbf{i}}$ is the linearized camera signals for each i$^{\text{th}}$ channel, α_i, β_i and γ_i are the gain, offset and gamma values for the ith channel, and $\mathbf{T}$ is a matrix with its column representing tristimulus values for each patch. The parameters of the GOG model and transformation matrix, $\mathbf{M}_\mathbf{c}$, are optimized to minimize the weighted sum of the mean and maximum CIEDE2000 color difference between measured, $\mathbf{T}$, and predicted tristimulus values, $\hat{\mathbf{T}}$, of the calibration target for a defined illuminant and observer. For a three-channel camera, $\mathbf{M}_\mathbf{c}$ is a (3 × 3) matrix, while for a 6-channel camera, $\mathbf{M}_\mathbf{c}$ is a (3 × 6) matrix. The raw camera signals are linearized to luminance factor, and no further linearization is required. However, it was found based on trial and error that incorporating parameters for the GOG model into the optimization process can achieve even higher colorimetric performance.

Finally, the matrix R method is used to combine both the spectral and colorimetric transformations. As illustrated in the left branch of the flowchart in Fig. 1, the multi-channel camera signals are converted to spectral reflectance factors, which in turn are used to calculate metameric blacks [Eqs. (1) and (4)]. On the right branch of the flowchart, the multi-channel camera signals are linearized and transformed to tristimulus values, from which the fundamental stimuli are calculated [Eq. (6)]. The final spectral reflectance, $\hat{\mathbf{N}}_\mathbf{c}$, is calculated combining the metameric blacks and fundamental stimuli:

$$\hat{\mathbf{N}}_\mathbf{c} = \mathbf{A}(\mathbf{A}'\mathbf{A})^{-1}\hat{\mathbf{T}} + \left(\mathbf{I} - \mathbf{A}(\mathbf{A}'\mathbf{A})^{-1}\mathbf{A}'\right)\hat{\mathbf{N}} \tag{12}$$

The matrix R method combines the benefits of both spectral and colorimetric transformations, so the method can provide high accuracy both spectrally and colorimetrically.

EXPERIMENTAL

The matrix R method was tested using a Sinarback 54H color-filter-array (CFA) digital camera. The camera has a Kodak KAF-22000CE CCD with a resolution of 5440 × 4080 pixels. The camera was modified in two ways. The built-in infrared cut-off filter in the camera was removed and replaced with clear glass. Second, a filter slider, holding two custom-designed absorption filters, was installed to collect two sequential sets of RGB images, producing six-channel camera images.[34] By design, one of two absorption filters had almost the same spectral transmittance as the removed Sinarback built-in infrared cut-off filter, so one of the RGB images could be used to simulate the production camera. Therefore, the performance of

TABLE I. Comparison of colorimetric performance (color difference CIEDE2000) between one colorimetric method of the production camera and two spectral reconstruction methods for the modified camera.

	Production camera			Pseudoinverse method			Matrix R method		
Targets	Mean	Max.	Std. Dev.	Mean	Max.	Std. Dev.	Mean	Max.	Std. Dev.
CCDC	1.9	10.9	1.9	1.4	13.3	1.6	0.9	3.2	0.7
CC	2.6	9.2	2.0	1.2	3.5	0.9	0.9	2.3	0.6
ESSER	3.3	13.2	2.3	1.3	5.4	0.9	1.2	4.1	0.8
Blue	4.5	12.5	2.9	3.2	10.0	2.1	2.5	7.8	1.5
Gamblin	3.0	10.7	2.3	2.0	4.1	0.9	1.8	4.0	0.9
Paintings	4.5	13.4	3.4	3.1	9.3	2.0	2.7	6.8	1.8
All targets	2.9	13.4	2.4	1.6	13.3	1.5	1.3	7.8	1.0

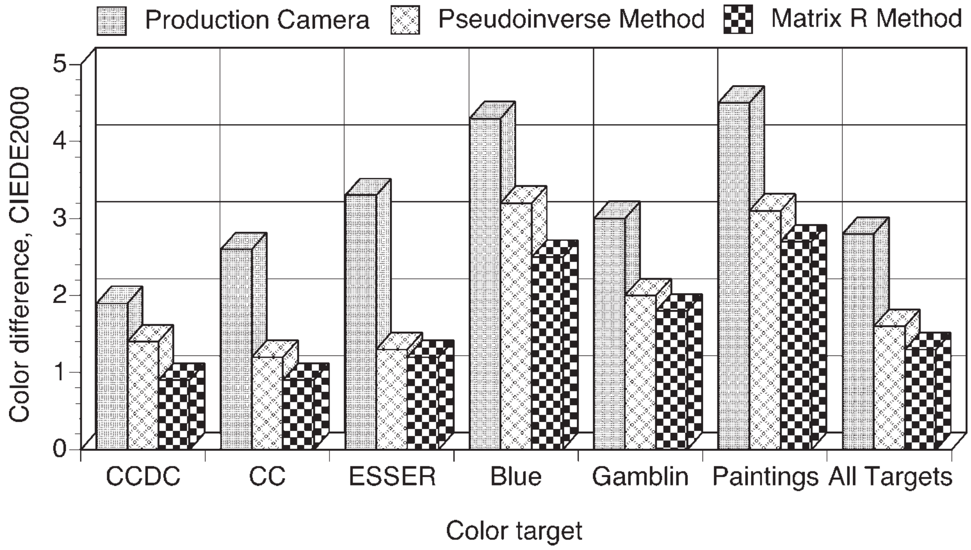

FIG. 2. Comparison of average CIEDE2000 color difference between one colorimetric method of the production camera and two spectral reconstruction methods for the modified camera.

the modified camera can be compared with the production camera.

The camera was set up perpendicular to the target. The lighting system included two Broncolor HMI F1200 sources, placed 45° on either side of the sample plane. For each position of the filter wheel, several targets were imaged: a dark field (to remove fixed-pattern noise), a uniform gray board (to compensate for lighting nonuniformity) and several color targets (to calibrate and verify the capture system). The calibration target was a GretagMacbeth ColorChecker DC (abbreviated as CCDC), and the verification targets include the Macbeth ColorChecker Color Rendition Chart (CC), the ESSER TE221 scanner target (ESSER), a custom target of Gamblin conservation colors (Gamblin), an acrylic-medium blue target (Blue) and two small oil paintings (Fish & Flower). Except for the two small oil paintings, the other targets were made up of a number of regular patches. These two paintings consisted of eleven Gamblin artist oil pigments. The eleven specific pigments were selected based on a statistical analysis of artist paints.[35–37] Just before finishing these paintings, each pure pigment was repainted on one of 11 selected positions on the surface, and those 11 marked positions for each painting were measured instead of the whole surface. The spectral reflectance factors of these targets were measured using a GretagMacbeth SpectroEye bidirectional spectrophotometer.

For each target, two RGB images were taken corresponding to the two custom-designed filters installed on the filter slider. Because of the movement of the slider, these two images were one-or-two-pixel misregistered and manually corrected using the simple registration tool in PhotoShop software. Then, the gray board was used for flat fielding to compensate for the nonuniformity of the illumination. To avoid pixel-to-pixel variation, the camera signals of these pixels on one patch of each target were averaged to represent those of the whole patch. The registered, flat-fielded, and averaged camera signals were then used to calibrate the target spectrally.

The linearity of the camera system was evaluated by comparing the averaged camera signals for the six neutral patches of the GretagMacbeth ColorChecker with their corresponding luminance factors. These camera signals fit reasonably well to a straight line since R-square values were close to unity. So no further linearization was required for this particular camera system in the generation of the spectral transformation. Even so, the gain, offset, and gamma parameters [Eq. (10)] were retained during the nonlinear optimization since the increased number of model parameters improved performance. The resulting gain, offset, and gamma parameters were quite close 1, 0, and 1, respectively, which further confirmed the linearity of the camera system.

RESULTS AND DISCUSSIONS

The colorimetric performance for both the production and modified cameras for illuminant D65 and the 1931 standard observer are listed in Table I and plotted in Fig. 2. For the production camera, Eqs. (10) and (11) were used, representing a model-based approach to building an ICC camera profile. For the modified camera, two methods were evaluated,

TABLE II. Spectral performance metrics comparing a conventional small aperture in-situ spectrophotometer with the predicted spectral image using the pseudoinverse method.

	RMS (%)			Metameric index (D65—Horizon, CIEDE2000)		
Targets	Mean	Max.	Std. Dev.	Mean	Max.	Std. Dev.
CCDC	1.6	4.0	0.6	0.7	7.6	1.0
CC	1.6	2.6	0.6	0.4	2.0	0.5
ESSER	1.9	6.8	1.0	0.5	5.1	0.6
Blue	3.6	10.0	2.1	1.4	7.3	1.6
Gamblin	2.8	8.5	1.5	0.6	2.4	0.6
Paintings	2.9	8.8	1.7	1.1	8.9	1.9
All targets	2.0	10.0	1.2	0.7	8.9	1.0

TABLE III. Spectral performance metrics comparing a conventional small aperture in-situ spectrophotometer with the predicted spectral image using the matrix R method.

Targets	RMS (%)			Metameric index (D65—Horizon, CIEDE2000)		
	Mean	Max.	Std. Dev.	Mean	Max.	Std. Dev.
CCDC	1.5	3.9	0.6	0.7	7.6	1.0
CC	1.6	2.6	0.6	0.4	2.0	0.5
ESSER	1.9	6.8	1.0	0.5	5.1	0.6
Blue	3.5	10.0	2.1	1.4	7.3	1.6
Gamblin	2.8	8.5	1.5	0.6	2.4	0.6
Paintings	2.9	8.7	1.7	1.1	8.9	1.9
All targets	2.0	10.0	1.2	0.7	8.9	1.0

the pseudoinverse method [Eqs. (8) and (9)] and the matrix R method [Eqs. (8)–(12)]. Except for the maximum color difference of the CCDC from the pseudoinverse method, the statistical results of CIEDE2000 color difference for the modified camera are superior to those for the production camera. It was expected that the modified camera would demonstrate better colorimetric accuracy than the production camera for both the calibration and verification targets since it used more channels. For the modified camera, the matrix R method achieved even higher colorimetric performance than the pseudoinverse method, and the maximum color differences for all the targets have been reduced significantly. The fact that matrix R achieved even higher colorimetric accuracy than the pseudoinverse method implies that the nonlinear optimization in the matrix R method is an effective technique to improve colorimetric performance, and the matrix R method takes advantage of this technique efficiently.

Tables II and III summarize the spectral performance metrics of the pseudoinverse and matrix R methods, including %RMS (root-mean-square) error and a metameric index that consists of a parameric correction[27] for illuminant D65 and CIEDE2000 color difference under Horizon illuminant with a correlated color temperature near 2200 K. Horizon was used since it is a common light source in museums. Because these two methods share the same metameric blacks obtained from the spectral transformation, the statistical results for the metameric index are, by definition, identical for these two methods. This level of performance is typical of this multi-filter RGB approach.[14]

In theory, the matrix R method should decrease spectral accuracy since tristimulus integration weights poorly approximate complex-subtractive colorants.[21] As the differences in tristimulus values increase between the two fundamental stimuli, the spectral differences become more pronounced. In this research, the matrix R method had minimal impact on spectral performance. This is likely a

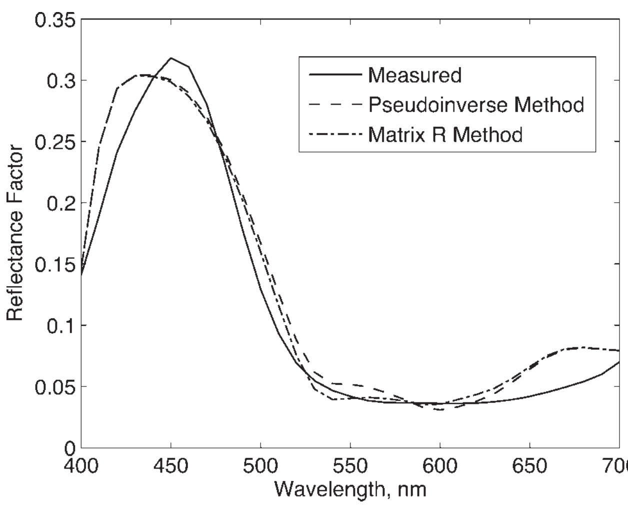

FIG. 3. Comparison of measured reflectance factor (solid line) with predicted ones from the pseudoinverse method (dashed line) and matrix R method (dash-dotted line). The color differences between measured and predicted reflectance factors from the pseudoinverse and matrix R methods are 3.2 and 0.8, respectively.

FIG. 4. The sRGB representation of the reconstructed multispectral image of a small oil painting with eleven marked spots made up of different pure pigments. 1: Indian Yellow 2: Cadmium Yellow Medium 3: Phthalocyanine Green 4: Titanium White 5: Ivory Black 6: Phthalocyanine Blue 7: Cobalt Blue 8: Cadmium Red Medium 9: Chromium Oxide Green 10: Quinacridone Red 11: Venetian Red.

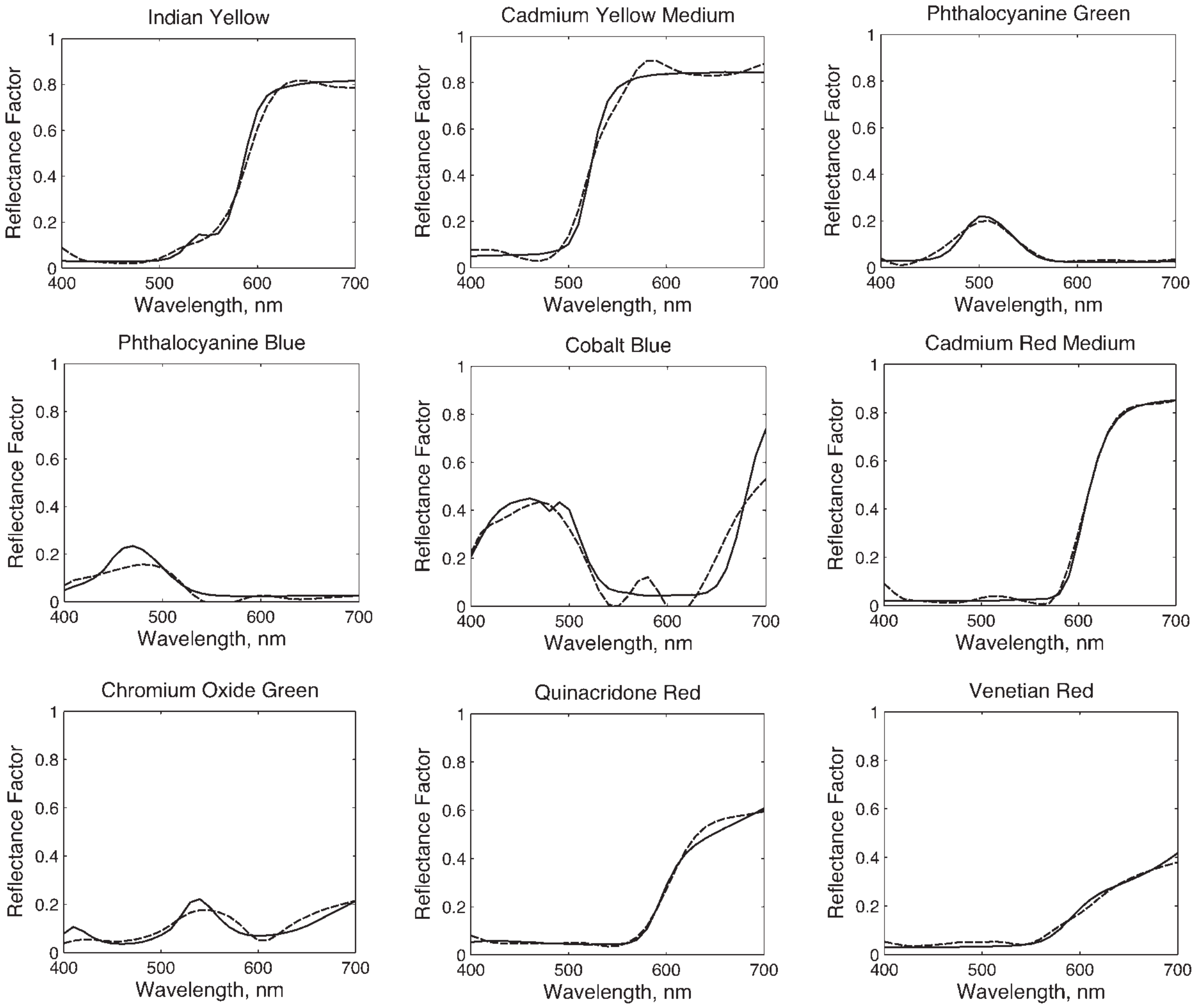

FIG. 5. Measured (solid line) and predicted (dashed line) spectral reflectance factors using the matrix R method. 1: Indian Yellow 2: Cadmium Yellow Medium 3: Phthalocyanine Green 4: Phthalocyanine Blue 5: Cobalt Blue 6: Cadmium Red Medium 7: Chromium Oxide Green 8: Quinacridone Red 9: Venetian Red.

result of the unconstrained nature of the spectral transformation and the sub-sampling of the visible spectrum with six channels resulting in spectra that are already spectrally selective. Furthermore, the tristimulus differences were not large. As a consequence, the spectral properties were not adversely affected. For example, the measured and predicted reflectances from these two methods for patch no. 13 (blue) of the GretagMacbeth ColorChecker are plotted in Fig. 3. The estimated spectrum from the pseudoinverse method undulates more than the measured spectrum. The matrix R method did not add further undulation. In this particular case, spectral performance improved. The value of the matrix R method is obvious when the color differences are compared between measured and predicted reflectances for the pseudoinverse and matrix R methods, 3.2 and 0.8, respectively. For this spectral imaging system, incorporating the fundamental stimuli from the optimized tristimulus values into the predicted reflectance factors from the pseudoinverse method did not diminish the spectral performance, but improved the colorimetric accuracy for a defined reference condition of illuminant and observer.

Two small oil paintings were also tested; one is a fish on a plate and the other is a bouquet of flowers in a blue vase. Figure 4 is the sRGB representation of the reconstructed multispectral image of the flower oil painting for CIE illuminant D65. The 11 points are also marked locating the pure pigments used to create this painting. The measured and predicted spectral reflectance factors for the nine chromatic pigments using the matrix R method are plotted in Fig. 5. For most of the pigments, the estimated spectra capture the dominant spectral characteristics with more spectral undulation. The exception is cobalt blue where the estimated spectrum is poor. Since the matrix R method is a learning-based reconstruction method, the performance will depend on the calibration target to a great extent. Recall that the ColorChecker DC was used as the calibration target. This target does not contain pigments with long wavelength reflectance "tails." In fact, the main pigment used to create blue green and blue colors is phthalocyanine blue, a cyan pigment whose reflectance factor is low throughout the red region of the spectrum. Evaluating Table III, there are two categories of performance. The first is the CCDC, CC, and ESSER targets, having average %RMS performance under 2.0. These targets do not contain blue colorants with long wavelength tails. The second category is the Blue, Gamblin, and Paintings targets, having average %RMS performance near 3.0. All of these targets contain pigments with long wavelength tails including cobalt blue and ultramarine blue. For this reason, it is a current research topic to develop a comprehensive calibration target that can cover the spectral variability of all typical artist paints.[35,36]

CONCLUSIONS

The image acquisition system, a modified commercial digital camera coupled with two filters, is a simple and practical spectral imaging system. This image system was tested with a new reconstruction method, the matrix R method. The new method is a learning-based reconstruction method, which depends on the calibration target. The method combines the benefits of both colorimetric and spectral transformations based on the Wyszecki hypothesis, where any stimulus can be decomposed into a fundamental stimulus and a metameric black. The colorimetric transformation is nonlinearly optimized to minimize the weighted color difference between measured and predicted tristimulus values for a certain viewing condition, and the predicted tristimulus values are used to form the fundamental stimulus. The spectral transformation is linearly optimized to minimize spectral RMS error between measured and predicted spectral reflectance factors, and the predicted spectral reflectance factor is used to calculate the metameric black. The final spectral reflectance factor combines the fundamental stimulus from the colorimetric transformation and the metameric black from the spectral transformation. The matrix R method takes advantage of both these transformations efficiently. Combining the fundamental stimuli from optimized tristimulus values with the predicted reflectances will not change the spectral performance, but can improve the colorimetric accuracy significantly for a certain viewing condition. The nonlinear optimization in the matrix R method is an effective technique to improve colorimetric performance. The method can achieve reasonable spectral accuracy, and at the same time higher colorimetric performance for a typical viewing condition. So it is a very promising method for building digital image databases for museums, archives and libraries.

There are several opportunities for improvement. The first is to replace the tristimulus integration weights used as additive primaries with primaries that better represent complex-subtractive colorants, as demonstrated by Li and Berns.[30] Matrix **R** is generalized as matrix **S**, [Eq. (7)], and matrix R method is defined by Eq. (13).

$$\hat{\mathbf{N}}_{\mathbf{c}} = \mathbf{E}(\mathbf{A}'\mathbf{E})^{-1}\hat{\mathbf{T}} + \left(\mathbf{I} - \mathbf{E}(\mathbf{A}'\mathbf{E})^{-1}\mathbf{A}'\right)\hat{\mathbf{N}} \tag{13}$$

A second opportunity is to improve upon the pseudoinverse transformation where the metameric black is estimated. One could constrain the transformation to improve smoothness, use a different optimization technique such as the Weiner inverse, or add a second step where the estimated spectrum is matched using apriori knowledge of the object's colorants. This was demonstrated for artist paints and the use of Kubelka-Munk turbid media theory as the mixing model.[32] This approach combined with image segmentation may enable the determination of concentration maps for each colorant used in a work of art. This is a current area of research.[38]

1. Berns RS. The science of digitizing paintings for color-accurate image archives: A review. J Imaging Sci Technol 2001;45:305–325.
2. Martinez K, Cupitt J, Saunders D, Pillay R. Ten years of art imaging research. Proc IEEE 2002;90:28–41.
3. Liang H, Saunders D, Cupitt J. A new multispectral imaging system for examining paintings. J Imaging Sci Technol 2005;49:551–562.
4. Ribés A, Schmitt F, Pillay R, Lahanier C. Calibration and spectral reconstruction for CRISATEL: An art painting multispectral acquisition system. J Imaging Sci Technol 2005;49:563–573.
5. Hardeberg JY, Schmitt F, Brettel H. Multispectral color image capture using a liquid crystal tunable filter. Opt Eng 2002;41:2532–2548.
6. Schmitt F, Brettel H, Hardeberg JY. Multispectral imaging development at ENST. In: Proceedings of the 1st International Symposium on Multispectral Imaging and Color Reproduction for Digital Archives, Chiba, Japan, 1999. p 50–57.
7. König F, Praefcke W. The practice of multispectral image acquisition. In: Proceedings of SPIE 3409 on Electronic Imaging: Processing, Printing and Publishing in Color, Zurich, Switzerland, 1998. p 34–41.
8. Hill B. Multispectral color technology: A way towards high definition color image scanning and encoding. In: Proceedings of SPIE 3409 on Electronic Imaging: Processing, Printing and Publishing in Color, Zurich, Switzerland, 1998. p 2–13.
9. Helling S, Seidel E, Biehlig W. Algorithms for spectral color stimulus reconstruction with a seven-channel multispectral camera. In: Proceedings of the 2nd European Conference on Colour Graphics, Imaging and Vision (CGIV 2004), Aachen, Germany, 2005. p 254–258.
10. Laamanen H, Jaaskelainen T, Hauta-Kasari M, Parkkinen J, Miyata K. Imaging spectrograph based spectral imaging system. In: Proceedings of the 2nd European Conference on Color Graphics, Imaging and Vision (CGIV 2004), Aachen, Germany, April 5–8, 2005. p 427–430.
11. Sugiura H, Kuno T, Watanabe N, Matoba N, Hayashi J, Miyata Y. Development of a multispectral camera system. In: Blouke MM, Sampat N, Williams GM, Yeh T, editors. Proceedings of SPIE 3965 on Sensors and Camera Systems for Scientific, Industrial and Digital Photographic Applications, SPIE, Bellinghan, WA, 2000. p 331–339.
12. Miyake Y, Yokoyama Y, Tsumura N, Haneishi H, Miyake K, Hayashi J. Development of multiband color imaging systems fro recordings of art paintings. In: Proceedings of SPIE 3648 on Color Imaging: Device-Independent Color, Color Hardcopy and Graphic Arts IV, San Jose, California, 1999. p 218–225.
13. Tominaga S. Multi-channel cameras and spectral image processing. In: Proceedings of the 1st International Symposium on Multispectral Imaging and Color Reproduction for Digital Archives, Chiba, Japan, 1999. p 18–25.
14. Berns RS. Color accurate image archives using spectral imaging. In: Proceedings of the National Academy Sciences (PNAS) in Scientific Examination of Art: Modern Techniques in Conservation and Analysis. National Academies Press; 2005. p 105–119.
15. Imai FH, Rosen MR, Berns RS. Comparison of spectrally narrow-band capture versus wide-band with a priori sample analysis for spectral reflectance estimation. In: Proceedings of the 8th Color Imaging Conference: Color Science and Engineering, Systems, Technologies, Applications. IS&T, Springfield, MA, 2000. p 234–241.

16. Imai FH, Berns RS, Tzeng D. A comparative analysis of spectral reflectance estimated in various spaces using a trichromatic camera system. J Imaging Sci Technol 2000;44:280–287.
17. Wyszecki G, Stiles WS. Color Science: Concepts and Methods, Quantitative data and Formulae, 2nd edition. New York: Wiley; 1982. p 184–187.
18. Wyszecki G. Valenzmetrische Untersuchung des Zusammenhanges zwischen normaler und anomaler Trichromasie, (Psychophysical investigation of relationship between normal and abnormal trichromatic vision). Farbe 1953;2:39–52.
19. Fairman HS. Recommended terminology for matrix R and metamerism. Color Res Appl 1991;16:337–341.
20. Cohen JB, Kappauf WE. Metameric color stimuli, fundamental metamers, and Wyszecki's metameric blacks. Am J Psychol 1982;95: 537–564.
21. Cohen JB, Kappauf WE. Color mixture and fundamental metamers: Theory, algebra, geometry, application. Am J Psychol 1985;98:171–259.
22. Cohen JB. Color and color mixture: Scalar and vector fundamentals. Color Res Appl 1988;13:5–39.
23. Cohen JB. Visual color and color mixture: the fundamental color space. Urbana, IL: University of Illinois Press; 2001. p xxv–xxvi.
24. Thornton WA. A critique of "recommended terminology for matrix R and metamerism" by Fairman HS. Color Res Appl 1991;16:361–363.
25. Imai FH, Rosen MR, Berns RS. Comparative study of metrics for spectral match quality. In: Proceedings of the 1st European Conference on Colour Graphics, Imaging, and Vision (CGIV 2002), Springfield, MA, 2002. p 492–496.
26. Sharma G. Digital color imaging handbook. Boca Raton: CRC Press; 2003. p 13–15.
27. Fairman HS. Metameric correction using parameric decomposition. Color Res Appl 1987;12:261–265.
28. Berns RS. Billmeyer and Saltzman's Principles of Color Technology, 3rd edition. New York: Wiley; 2000. p 128, 212.
29. Imai FH, Berns RS. High-resolution multi-spectral image archives: A hybrid approach. In: Proceedings of the 6th Color Imaging Conference: Color Science, Systems and Applications, Springfield, VA, 1998. p 224–227.
30. Li Z, Berns RS. Comparison of methods of parameric correction for evaluating metamerism. Color Res Appl 2007;32:293–303.
31. Derhak M, Rosen M. Spectral colorimetry using LabPQR—An interim connection space. In: Proceedings of the 12th Color Imaging Conference: Color Science, Systems, Applications, IS&T, Springfield, VA, 2004. p 246–250.
32. Zhao Y, Berns RS, Okumura Y, Taplin LA. Improvement of spectral imaging by pigment mapping. In: Proceedings of the 13th Color Imaging Conference: Color Science and Engineering, Systems, Technologies and Applications, IS&T, Springfield, VA, 2005. p 40–45.
33. Berns RS, Katoh N. Methods of characterizing displays. In: Green P, MacDonald LW, editors. Color Engineering: Achieving Device Independent Colour. New York: Wiley; 2002. p 127–164.
34. Taplin LA, Berns RS. Practical spectral capture systems for museum imaging. In: Proceedings of the 10th Congress of the International Colour Association AIC Colour 05, Granada, Spain, 2005. p 1287–1290.
35. Mohammadi M, Nezamabadi M, Berns RS, Taplin LA. A prototype calibration target for spectral imaging. In: Proceedings of the 10th Congress of the International Colour Association AIC Colour 05, Granada, Spain, 2005. p 387–390.
36. Mohammadi M, Nezamabadi M, Berns RS, Taplin LA. Spectral imaging target development based on hierarchical cluster analysis. In: Proceedings of the 12th Color Imaging Conference: Color Science and Engineering, systems, Technologies and Applications, IS&T, Springfield, VA, 2004. p 59–64.
37. Mohammadi M, Nezamabadi M, Taplin LA, Berns RS. Pigment selection using Kubelka-Munk turbid media theory and non-negative least square technique. MCSL Technical Report, 2004. Available at http://www.art-si.org [Accessed September 22, 2006].
38. Zhao Y, Berns RS, Taplin LA. Image segmentation and pigment mapping in spectral imaging. In: Proceedings of the 6th International Congress of Imaging Science, Rochester, USA, 2006. p 294–297.